LWT - Food Science and Technology 191 (2024) 115609

Contents lists available at ScienceDirect

LWT

journal homepage: www.elsevier.com/locate/lwt

Linear and nonlinear viscoelasticity of edible o/w emulsions used as saturated fat replacers

M. Espert [a,*], C. Gracia-Fernández [b], A. Salvador [a], T. Sanz [a], M.J. Hernández [c]

[a] Group of Physical and Sensory Properties of Food, Institute of Agrochemistry and Food Technology, 46980, Paterna (Valencia), Spain
[b] TA Instruments Waters Chromatography, Tres Cantos, 28760, Madrid, Spain
[c] Department of Earth Physics and Thermodynamics, Faculty of Physics, University of Valencia, 46100, Burjassot, Valencia, Spain

ARTICLE INFO

Keywords:
Rheology
Large amplitude oscillation shear
Emulsion
Methyl cellulose
Hydroxypropyl methylcellulose

ABSTRACT

A recent strategy for controlling saturated fat intake consists on the design of vegetable oil-based emulsions. The aim was to characterize the linear and nonlinear viscoelastic properties of o/w emulsions formulated with two types of cellulose: MX (methylcellulose, MC) and F4M (hydroxypropyl methylcellulose, HPMC). The emulsions were characterized by steady flow curves and frequency sweeps in SAOS (Small Amplitude Oscillatory Shear) regime. In order to evaluate linear and non-linear response, strain sweeps were performed from 0.01 to 1000% strain amplitude at different frequencies (0.1, 1 and 5 Hz). Fourier Transform rheology and orthogonal stress decomposition were applied and LAOS (Large Amplitude Oscillatory Shear) parameters (G'_M, G'_L, η'_M, η'_L, S and T) were analysed. The type of cellulose ether significantly affected both flow behaviour and internal structure of the samples. MX emulsion presented greater consistency at rest and higher gel strength in SAOS regime with a lower frequency dependence than F4M emulsion. However, both emulsions presented similar properties at large deformations, showing shear thinning and strain stiffening behaviour. Nonlinear viscoelastic analysis allows to improve the textural characterization of emulsions, providing complementary useful information for establishing the most suitable formulation in experimental conditions closer to real applications and processes.

1. Introduction

Structured emulsions are soft-solid materials with good physical stability and viscoelastic mechanical properties, in which emulsified droplets are entrapped within a gel matrix (Li et al., 2021). This type of emulsions shows practical applications in food, pharmaceutics, and cosmetics, since they can provide stability and a solid-like functionality to fat-containing products (Jiang et al., 2019).

Cellulose derivatives have been successfully used in stabilizing emulsions which attracts extensive interests for "surfactant-free" emulsions with high physical stability (Jiang et al., 2019). Cellulose chemical structure, i.e. the number of hydroxypropyl and methoxyl groups and molar substitution plays a relevant role in emulsion stability (Shimada, Fonseca, & Petri, 2017), hydration capacity (Arai & Shikata, 2017), digestibility of fat in emulsion matrix (Espert et al., 2017) and mechanical and rheological properties (Espert et al., 2017; Sanz, Falomir, & Salvador, 2015). Different cellulose ethers have been demonstrated to be suitable for reduced-fat food, including direct application as fat replacer additive to the food matrix or its application as structuring unsaturated fat agent in emulsions and oleogels to replace saturated fat (Gibis, Schuh, & Weiss, 2015; Laguna, Primo-Martín, Varela, Salvador, & Sanz, 2014; Lee, 2018; Martínez-Cervera, Salvador, & Sanz, 2015), while conferring good sensory acceptability (Borreani, Hernando, Salvador, & Quiles, 2017; Espert, Bresciani, Sanz, & Salvador, 2019; Espert, Hernández, Sanz, & Salvador, 2021; Tarancón, Fiszman, Salvador, & Tárrega, 2013).

Rheological characterization of emulsions is an essential tool to provide fundamental information about the structural stabilization and interactions of the components within emulsions (McClements, 2009). Small amplitude oscillatory shear testing (SAOS), as a non-destructive rheological technique, has been one of the most widely used rheological methods to study the linear viscoelastic properties of a wide range of materials (Gunasekaran & Ak, 2000). In these tests, the response of the material is observed in the linear viscoelastic region (LVR), i.e., at small deformations, without significantly altering the structure. However, most food materials are subjected to higher deformations in processing operations or oral processing. Therefore, it is necessary to perform large amplitude oscillatory shear tests (LAOS) which provide information

* Corresponding author. Group of Physical and Sensory Properties of Food, Institute of Agrochemistry and Food Technology, 46980, Paterna (Valencia), Spain.
E-mail address: mespert@iata.csic.es (M. Espert).

https://doi.org/10.1016/j.lwt.2023.115609
Received 7 September 2023; Received in revised form 27 November 2023; Accepted 30 November 2023
Available online 4 December 2023

about nonlinear rheological properties. This means a more detailed understanding of the rheological behaviour of food under real application conditions, what may not be visible through SAOS measurements (Melito, Daubert, & Foegeding, 2012; Van den Berg, Van Vliet, Van der Linden, Van Boekel, & Van de Velde, 2007; Yazar, Duvarci, Erturk, & Kokini, 2019), although LAOS tests results are more difficult to interpret.

The study of non-linear viscoelastic properties can also be related to the droplet size of emulsions providing useful insight into their stability (Reinheimer, Grosso, Hetzel, Kübel, & Wilhelm, 2012). Furthermore, LAOS experiments provide insight into how structure and structural changes influence the texture and decomposition of food during chewing, correlating therefore with the sensory perception (Melito, Daubert, & Foegeding, 2013). In particular, this is necessary to ensure the suitability of any system as a fat mimetic (Marangoni, Van Duynhoven, Acevedo, Nicholson, & Patel, 2020).

Over the last years LAOS tests has been used for the characterization of many structured food materials such as foams, concentrated emulsions, gels, chocolate, and different types of dough (Duvarci, Yazar, & Kokini, 2017; Li et al., 2021). Within emulsions and gels, systems with hydrocolloids such as gums, gelatin and their combination have been studied (Anvari & Joyner, 2017), but concentrated emulsions with cellulose ethers have not been investigated to date.

The objective of the current study was to characterize both linear and nonlinear viscoelastic properties of o/w emulsions formulated with two types of cellulose ether, recognized as edible saturated fat substitute. Since the different chemical structure of the cellulose ethers may have influence in the emulsion structure characteristics, it is necessary to analyse their response when applying experimental conditions that better simulate real processing conditions, both in flow and shear deformations.

2. Materials and methods

2.1. Preparation of emulsions

Different o/w emulsions were prepared using two cellulose ethers: METHOCEL™ MX and METHOCEL™ F4M (The Dow Chemical Company, Midland, MI, USA). These present different chemical substitutions: MX is a methyl cellulose (>30.0% methoxyl) and F4M is a hydroxylpropylmethyl cellulose (29% methoxyl, 6.2% hydroxypropyl). This difference results in/leads to a different viscosity: F4M has a viscosity of 4000 mPa s and MX has a viscosity of 50 000 mPa s (20 g/L aqueous solution at 20 °C measured by The Dow Chemical Company following reference methods ASTM D1347 and ASTM D2363) (Ethers, 1997).

Emulsions were prepared using the following proportions: 470 (g/kg) sunflower oil (Koipe Sol, Deoleo S.A., Córdoba, Spain) 20 (g/kg) cellulose ether and 510 (g/kg) water.

At first, cellulose ether was dispersed in sunflower oil using a Heidolph stirrer (Heidolph Instruments GmbH & Co. KG, Schwabach, Germany) at 280 rpm (29.3 rad/s) for 5 min. Then the mixture was hydrated by gradually adding of water at 1 °C while continuous stirring. A water temperature of 1 °C was selected according to the specific hydration requirement of MX cellulose (the highest methoxyl content) and then it was also used for the other cellulose types. Finally, the emulsion was homogenized using an Ultra-Turrax T18 homogenizer (IKA, Staufen, Germany) at 6500 rpm (680.7 rad/s) for 15 s and at 17500 rpm (1832.6 rad/s) for 60 s.

Three different batches of both emulsions were prepared in different days.

2.2. Rheological measurements

All rheological measurements were carried out using a controlled stress rheometer (AR-G2, TA Instruments, Crawley, England)). A 40 mm roughened parallel plate geometry was used, setting a gap of 1 mm. By using an advanced Peltier system, temperature was fixed at 20 °C for all trials, remaining 5 min of equilibration before each test. At least two replicates of all rheological measurements were performed on each of the three emulsion batches prepared.

Stepped flow curves were performed in controlled stress mode, in an interval of shear rates including Newtonian plateau up to shear rates about 100 s^{-1}. Stress varied from 1 to 600 Pa, in logarithmic distribution with 10 points per order of magnitude and 30 s per point.

The simplified Carreau model (Mezger, 2020) was satisfactorily fitted to viscosity values as a function of shear rate data (Eq. (1)):

$$\eta = \frac{\eta_0}{\left(1 + \left(\frac{\dot{\gamma}}{\dot{\gamma}_c}\right)^2\right)^s} \quad (1)$$

where η_0 is the zero-shear viscosity, $\dot{\gamma}_c$ is the critical shear rate, and s in an adimensional parameter related to shear thinning character.

Frequency sweep tests from 0.01 to 10 Hz were carried out at 0.5 Pa (within the linear viscoelastic region, LVR).

Strain sweeps experiments were performed from 0.01 to 1000% strain amplitude at different frequencies (0.1, 1 and 5 Hz).

2.3. Fourier transform rheology

In order to evaluate linear and non-linear response, Fourier Transform rheology and orthogonal stress decomposition (Ewoldt, Hosoi, & McKinley, 2009) were applied on raw waveform data strain.

Lissajous-Bowditch plots, both elastic and viscous curves, were analysed for the three frequencies considered and three values of strain (1, 100 and 1000%).

Elastic modulus was separated into *minimum strain elastic modulus*, G'_M, and *large strain elastic modulus*, G'_L, defined in Eq. 2

$$G'_M = \left.\frac{d\sigma}{d\gamma}\right|_{\gamma=0} \quad G'_L = \left.\frac{\sigma}{\gamma}\right|_{\gamma=\gamma_{max}} \quad (2)$$

Dynamic viscosity was converted to instantaneous viscosity at minimum shear rate named *minimum strain rate viscosity*, η'_M, and instantaneous viscosity at maximum shear rate, named *large strain rate viscosity*, η'_L, defined in Eq. (3) and (4)

$$\eta'_M = \left.\frac{d\sigma}{d\dot{\gamma}}\right|_{\dot{\gamma}=0} \quad \eta'_L = \left.\frac{\sigma}{\dot{\gamma}}\right|_{\dot{\gamma}=\dot{\gamma}_{max}} \quad (3)$$

Strain-hardening (S) and shear-thickening (T) ratios were calculated from the Chebyshev coefficients obtained by Fourier transform analysis for all applied strain amplitudes. These ratios are related to the above moduli and viscosities (Eq. (4) and (5))

$$S = \frac{G'_L - G'_M}{G'_L} \quad (4)$$

$$T = \frac{\eta'_L - \eta'_M}{\eta'_L} \quad (5)$$

2.4. Data analysis

The raw data obtained were processed using TRIOS 5.4 software (TA Instruments, USA).

One-way analysis of variance (ANOVA) tests were done using XLSTAT software system (2019.2.2). The least significant differences (LSD) were calculated using the Fisher's test, assuming that differences among the samples were significative when $p < 0.05$.

3. Results and discussion

3.1. Flow curves

Viscosity as a function of shear rate are plotted in Fig. 1. Continuous lines correspond to simplified Carreau model (Eq. (1)) fitting the experimental data. Flow curves of both emulsions showed two different regions. The first one, at low shear rates showed a Newtonian region with a plateau of constant viscosity, the zero-shear viscosity, η_0. However, at higher shear rates, the flow curves presented a decrease in viscosity when increasing shear rates, indicating a shear thinning behaviour. As expected, the type of cellulose ether affected the steady shear viscosity, particularly at lower shear rates. MX emulsion presented zero-shear viscosity values which were two orders of magnitude greater than the corresponding values of F4M emulsion viscosity (43947 ± 11370 Pa s for MX and 1342 ± 357 Pa s for F4M). This difference in zero-shear viscosity is related to the consistency of the emulsions at rest, observed in the images shown in Fig. 2, what reproduces the results obtained for hydrated cellulose ether solutions (Espert et al., 2017).

At high shear rates, corresponding to oral and industry processing such as chewing, swallowing, mixing, spreading (Barnes, 2000), viscosity values were comparable in both emulsions. However, the two emulsion showed a different shear-thinning behaviour as indicated in their *s* index values obtained when fitting to Carreau model. MX emulsion presented a stronger shear thinning behaviour, with s = 0.425 ± 0.010, while F4M emulsion was s = 0.285 ± 0.007.

The greatest consistency of MX emulsion at rest could be attributed to its higher methoxyl content whant implies a higher molecular weight. Longer chains experienced greater entanglement levels, being capable of offering higher resistance to flow (Otoni, Lorevice, de Moura, & Mattoso, 2018). The shear rate orients the biopolymer chains in the direction of flow, leading to a decrease in the number of entanglements when increasing shear rate. The decrease is expected to be very similar when the biopolymer concentrations are comparable. However, the studied emulsions presented significant differences, which could be due to the role of the interface. Higher molecular weight molecules could generate higher steric repulsion, leading to an increase in the viscosity of the Newtonian plateau. However, this would be irrelevant when the interface rupture occurs at high deformation rates.

As a consequence of the differences in zero shear and s index, the viscosity drop was also produced at lower shear rates for the MX emulsion. That was related to the critical shear rate, γ_C, that was 0.003 ± 0.001 s^{-1} for the MX emulsion, while for F4M emulsion the viscosity plateau extended until larger shear rates, with a critical shear rate one order of magnitude higher, $\gamma_C = 0.021 \pm 0.009\ s^{-1}$.

3.2. Mechanical spectra at small strain amplitudes

The two tested emulsions also disclosed a different viscoelastic behaviour in frequency sweeps performed in SAOS regime (Fig. 1B) as it was shown in the previous work by Espert et al. (2017). MX emulsion showed an elastic-dominant behaviour (G' > G″) with a moderate frequency dependence in this frequency range, what corresponds to a weak gel behaviour in the rubbery plateau region (Barnes, 2000). On the contrary, F4M emulsion exhibited high dependence on frequency. The mechanical spectra were in the terminal and transition region, typical of entanglement solutions (Barnes, 2000). At low frequencies G″ values were higher than G′, indicating a liquid-like character, while at higher frequencies emulsion behaviour changed into elastic solid-like. The crossover point, G′ = G″, corresponded to a modulus of 131 ± 6 Pa for a frequency of 0.126 ± 0.004 Hz (corresponding to 0.79 ± 0.03 rad/s and a relaxation time of 1.27 s).

Comparison of the two emulsions mechanical spectra suggested that their internal structure was quite different. Previous works showed a strong correlation between the type of cellulose ether used and the resulting mechanical strength (Espert et al., 2017; Borreani et al., 2017; Sanz et al., 2015). The higher structure complexity in MX emulsion is presumably associated to the higher molecular weight and to the higher methoxyl content, which further increase cellulose hydrophobicity (Sanz et al., 2015). For the same concentration, the number of molecules that could be adsorbed by a droplet would be higher for polymers with higher molecular weight.

Microscopic images taken in a previous work (Espert et al., 2017) confirmed the differences in the internal structure. MX emulsion consisted of globules that were approximately twice the size of those of the F4M emulsion. This resulted in the MX emulsion having a more solid character, as evidenced by its more compact and consistent visual appearance in the beaker (Fig. 2).

3.3. Oscillatory strain sweeps

Oscillatory strain sweep tests were performed over a wide

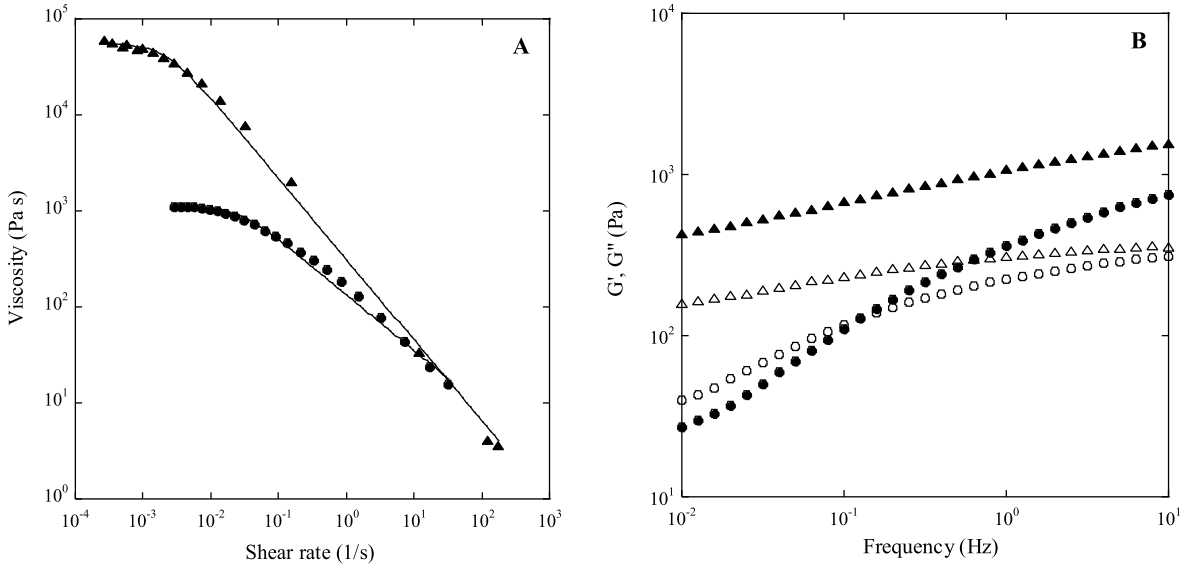

Fig. 1. Flow curves and mechanical spectra for the two emulsions studied. ●: Hydroxypropyl methylcellulose (F4M); ▲: Methylcellulose (MX). **A**: Shear-rate dependence of viscosity. **B**: Storage modulus (G: filled symbols) and loss modulus (G″: open symbols) in linear viscoelastic region, as a function of frequency.

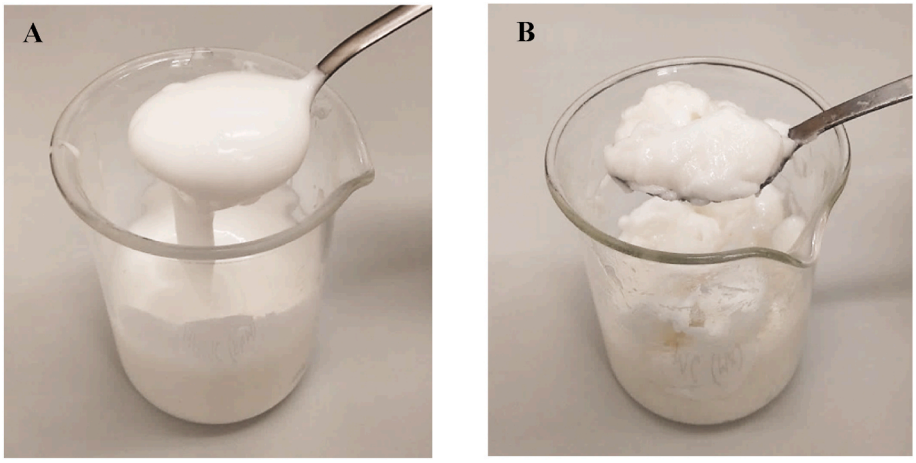

Fig. 2. Visual appearance of the emulsions studied. **A**: Hydroxypropyl methylcellulose (F4M); **B**: Methylcellulose (MX).

deformation strain amplitude range from 0.01 to 1000%. Considering the highly frequency dependent response of F4M emulsion (Fig. 1B), three different frequencies were chosen for further analysis of strain response of viscoelastic moduli: 0.1 Hz, 1 Hz and 5 Hz. A lower frequency of 0.05 Hz, in the terminal region of mechanical spectra, with G"$>$G' was initially considered, but experimental problems with the rheometer did not make it possible, so the minimum frequency was set to 0.1 Hz, close to the cross-over point. Fig. 3 illustrates the dependence of G' and G'' with strain amplitude at the three frequencies considered. The curve shape of these amplitude sweeps corresponded to the type I, according to Hyun et al. (2011) classification, what indicates strain thinning regardless the oscillation frequency (Wang & Selomulya, 2022).

Mean values of the constant storage modulus (G'_0) and loss tangent (tan δ_0) corresponding to the plateau were calculated in order to characterize the linear viscoelastic region, LVR. These parameters are shown in Table 1, where the statistical differences with frequency for each emulsion were analysed.

As indicated above, MX emulsion showed higher network rigidity, since G'_0 values are greater at all frequencies tested. Statistical differences with frequency were more noticeable in the case of the F4M emulsion, as it was expected from Fig. 1B. Regarding the viscoelastic character, the lower values of loss tangent indicated a stronger solid-like behaviour of MX emulsions. In addition, a decrease of tan δ was observed as the frequency increases. As expected, while in the MX emulsion the tan δ values were similar, in the F4M emulsion significant differences were observed at the different frequencies studied. At the lowest frequency considered, the tan δ value for F4M emulsion was approximately 1, indicating closeness to liquid-like behaviour (Razavi, Alghooneh, Behrouzian, & Cui, 2016), since this frequency was near to the cross over point (Fig. 1B).

However, both moduli decreased when increasing strain amplitude above a critical value, so the emulsions were out of the linear viscoelastic region. To determine the extent of the LVR, yield point was calculated considering a deviation of 5% of the plateau (Mezger, 2020). Values of yield stress (σ_y) and the corresponding strain (γ_y) are also presented in Table 1. They are considered to measure the starting point of the gel strength weakening (Yousefi & Razavi, 2015). The end of the LVR corresponded to a similar deformation for both samples, about 10%. For F4M emulsion no significant differences in γ_y were found, while in the case of MX, as the frequency increased, the γ values slightly increased. However, when considering the yield stress, the dependence on frequency were more significant. On addition, important differences were shown between emulsions, as MX needed higher values of stress to

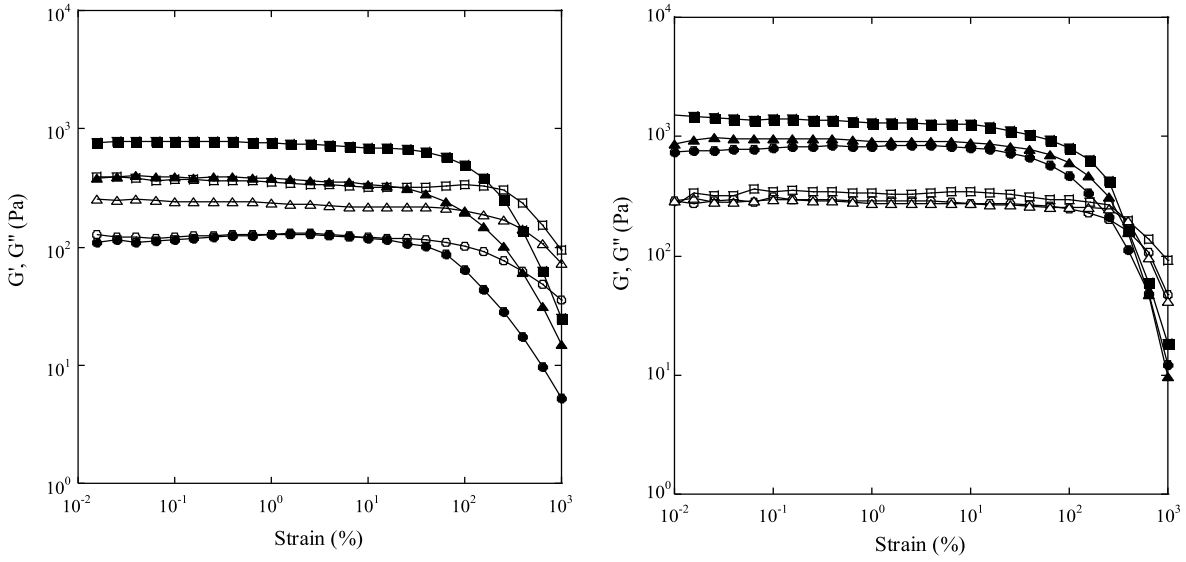

Fig. 3. Storage modulus (G': filled symbols) and loss modulus (G'': open symbols) as a function of oscillatory strain amplitude at the different frequencies studied (● 0.1 Hz, ▲1 Hz, ■5 Hz). **A**: Hydroxypropyl methylcellulose (F4M); **B**: Methylcellulose (MX).

Table 1
Mean values of parameters characterizing strain sweeps for the two types of emulsions studied (F4M: hydroxypropyl methylcellulose; MX: methylcellulose). G_0' and δ_0 correspond to storage modulus and loss angle for the plateau region in the linear viscoelastic region (LVR) and γ_y, γ_f, σ_y, σ_f are the strains and stresses in the yield point and the flow point. LSD are the least significant differences (n = 6).

Emulsion	Frequency (Hz)	LVR-Yield point				Flow point		
		G_0' (Pa)	tan δ_0	γ_y(%)	σ_y (Pa)	G' = G" (Pa)	γ_f (%)	σ_f (Pa)
F4M	0.1	128^{C}	0.98^{A}	10^{A}	18^{C}	125^{C}	8^{C}	15^{C}
	1	408^{B}	0.62^{B}	8^{A}	35^{B}	219^{B}	93^{B}	291^{B}
	5	775^{A}	0.47^{C}	12^{A}	122^{A}	314^{A}	198^{A}	883^{A}
LSD		90	0.08	9	15	43	7	83
MX	0.1	732^{B}	0.345^{A}	6^{C}	60^{C}	182^{A}	285^{A}	732^{B}
	1	946^{B}	0.288^{AB}	10^{B}	93^{B}	210^{A}	320^{A}	966^{C}
	5	1287^{A}	0.259^{B}	15^{A}	190^{A}	237^{A}	336^{A}	1159^{A}
LSD		242	0.06	0.03	22	69	58	172

^{ABC} For each emulsion, different letters in each column indicate significant differences between the means ($p < 0.05$) according to Fisher's test.

reach the same deformation. This fact could be related to the flow behaviour observed in Fig. 1A. The exit of the Newtonian zone in the F4M emulsion occurred at about 10 Pa, while the MX emulsion needed stress values one order of magnitude higher (about 100 Pa).

Out of the LVR, at high strain values of the amplitude sweep a well-defined flow point, where G' = G″ was observed in Fig. 3. Table 1 shows the values of strain and corresponding stress(γ_f, σ_f), and the moduli for these points. No significant differences appeared in the MX emulsion, so this flow point turned to be independent of the frequency applied. However, in F4M emulsion the flow point was highly dependent on frequency. This point appeared at higher strains (and stresses) as the frequency increased and corresponded to higher moduli values. The maximum strain the MX sample could hold before the structure breakdown in the interface was not dependent of the amount of time the oscillatory strain was applied, but corresponded to an instantaneous rupture occurring at different times.

3.4. Lissajous-Bowditch curves

This transition from linear to nonlinear behaviour may be qualitatively investigated by analyzing the shapes of the Lissajous-Bowditch plots (Hong et al., 2019; Joyner & Meldrum, 2016; Szopinski & Luinstra, 2016). Tables 2 and 3 show a graphical representation of the total stress response as a function of strain (elastic Lissajous-Bowditch curve) and as the total stress as a function of strain-rate (viscous Lissajous-Bowditch curve) of both emulsions. They show separately the elastic and the viscous stress contributions, represented by the dashed lines inside the continuous closed loops.

In order to visualise differences between different regions in amplitudes sweeps, three values of strain have been chosen (1, 100 and 1000%). Observing Figs. 3 and 1 % strain was in SAOS (small amplitude oscillatory shear) regime, within the LVR, before yield point. The strain value of 1000 % was in LAOS (large amplitude oscillatory shear) regime, clearly in non linear region, with G"$>$G'. In addition, a strain of 100 % was also chosen, considering that it was in MAOS (medium amplitude oscillatory shear) regime, as this strain was around the flow point. This region is defined as a transition domain between SAOS and LAOS regimes (Coblas, Broboana, & Balan, 2016).

In both emulsions, for 1% strain the elliptical shape of the loops and the straight lines of the elastic and viscous contributions confirmed the expected results for LVR in SAOS. Shapes of stress versus strain rate curves (Tables 2 and 3) were quite similar in both type of emulsions for

Table 2
Normalized elastic (stress-strain) and viscous (stress-strain rate) Lissajous-Bowditch curves for emulsion containing hydroxypropyl methylcellulose (**F4M)** at the strain amplitudes (1, 100 and 1000 %) and frequencies (0.1, 1 and 5 Hz) considered. Continuous line**:** Total stress, dashed line: elastic stress and viscous stresses.

	$\sigma/\sigma_{max} = f(\gamma/\gamma_{max})$			$\sigma/\sigma_{max} = f(\dot{\gamma}/\dot{\gamma}_{max})$		
	1%	100%	1000 %	1%	100%	1000 %
0.1 Hz		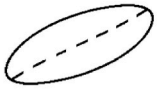		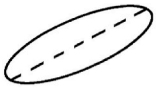	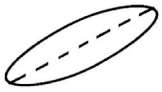	
1 Hz	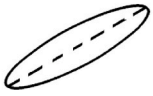			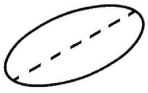	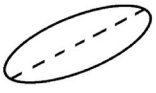	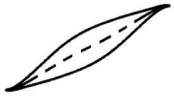
5 Hz	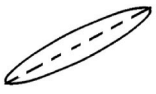	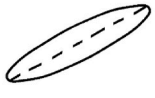				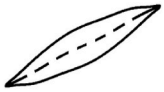

Table 3
Normalized elastic (stress-strain) and viscous (stress-strain rate) Lissajous-Bowditch curves for emulsion containing methylcellulose **(MX)** at the strain amplitudes (1, 100 and 1000 %) and frequencies (0.1, 1 and 5 Hz) considered. Continuous line: Total stress, dashed line: elastic stress and viscous stresses.

	$\sigma/\sigma_{max} = f(\gamma/\gamma_{max})$			$\sigma/\sigma_{max} = f(\dot{\gamma}/\dot{\gamma}_{max})$		
	1%	100%	1000 %	1%	100%	1000 %
0.1 Hz						
1 Hz						
5 Hz	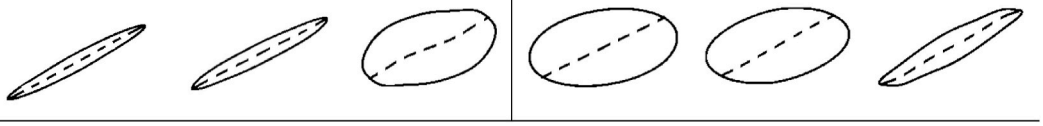					

this deformation. However, differences were observed in stress versus strain, since enclosed areas of the loops were smaller in MX emulsion, particularly at higher frequencies. That means phase angles for MX emulsion were lower than F4M emulsions, indicating more elastic-dominant behaviour (Li et al., 2021), corroborated by the fact that total stress was closer to elastic stress (dashed line in Table 3).

Although 100% strain corresponding to the MAOS zone is considered to be outside the LVR, no significant differences in Lissajous curves shapes were observed, both in elastic and viscous contributions.

However, at 1000% strain (LAOS) elliptical shape and linearity of the elastic and viscous contributions was clearly lost, highlighting the expected nonlinear behaviour.

Elastic Lissajous plots of the different emulsions at 1000% strain showed that total stress figures stretched horizontally and flattened vertically becoming a parallelogram with a rounded edge (Hong et al., 2019), thus increasing the area enclosed by the curve. That indicates an enhanced viscous dissipation and a transition from elastic-dominated to viscous-dominated behaviour. This change could be related to the microstructural permanent deformations and the shear thinning behaviour in emulsions flow (Hong et al., 2022). The curvature in elastic stress (dashed line) was indicative of strain stiffening behaviour (Etwold, Hosoi & McKinley, 2009), as elastic stress increases when increasing strain, presenting an upturn line (Aguilar-Zárate, Macias-Rodriguez, Toro-Vazquez, & Marangoni, 2019; Li et al., 2021).

Viscous Lissajous plots for 1000% strain showed the total stress loop was closer to the viscous stress part, so the enclosed areas were smaller. The shape was deformed, as it was clearly not elliptical and tended to a S shape for lowest frequencies, typical of a predominantly viscous non-linear behaviour (Etwold, 2008; Szopinski & Luinstra, 2016; Yazar et al., 2019; Li et al., 2021). The viscous stress curvature indicated a shear thinning behaviour, what was better observed for the lowest frequency.

Although visual evaluation of Lissajous plots is helpful to have an outline of non-linear viscoelastic response, quantitative methods are further necessary for analyzing the non-linear behaviour. As indicated above, for large deformations, out of the linear region, the stress output measured was observed not to be purely sinusoidal. This behaviour cannot be described in terms of a storage modulus (G′) and loss modulus (G″), due to the presence of higher harmonic contributions (Hyun et al., 2011). Ewoldt, Hosoi, and McKinley (2008) developed a technique to quantify the extent and type of nonlinear behaviour shown in these Lissajous plots, by using two G'_M and G'_L moduli and two instantaneous viscosities, η'_M and η'_L (Faber, Van Breemen, & McKinley, 2017; Joyner & Meldrum, 2016; Szopinski & Luinstra, 2016). G'_M and G'_L moduli (Eq. (2)) correspond to the slope of the tangent of elastic stress at minimum strain ($\gamma = 0$) and the slope of the secant at maximum strain ($\gamma = \gamma_{max}$) respectively. η'_M and η'_L viscosities (Eq. (3)) correspond to the tangent of viscous stress at minimum shear rate ($\dot{\gamma} = 0$) and the slope of the secant at maximum strain ($\dot{\gamma} = \dot{\gamma}_{max}$) respectively.

The ratio of the new elastic moduli (G_L'/G_M') can be used to indicate strain hardening ($G_L'/G'_M > 1.10$) and softening ($G_L'/G'_M < 0.90$) behaviour, while the ratio of the instantaneous viscosities was used to indicate shear thinning ($\eta'_L/\eta'_M < 0.90$) and thickening ($\eta'_L/\eta'_M > 1.10$) behaviour (Anvari & Joyner, 2017; Ewoldt et al., 2009; Melito, Daubert, & Foegeding, 2012).

Those ratios for the three frequencies and three values of strain considered are shown in Table 4. Both emulsions generally showed linear viscoelastic behaviour ($0.90 < G_L'/G'_M < 1.10$) at 1% strain in all the frequencies studied and not significant differences were shown for 100 % strain. These results confirm the shape of the elastic Lissajous plots (Tables 2 and 3), as tangent and secant lines in the ellipses had similar slopes.

For 1000% strain the ratios G'_L/G'_M were >1.10 in all cases, what could be considered as indicative of strain hardening behaviour, also suggested by the curvature in the elastic stress in Lissajous curves. Values of these ratios were higher for the lower frequencies. At these frequencies the material was more relaxed, so chains at the interface had time to build up a structure when applying strain and thus reinforce it, which could be the reason of this strain hardening behaviour.

Regarding to η'_L/η'_M, significant differences were only found for 1000% strain in F4M emulsions, although the distortion of the Lissajous plots were clear in both emulsions. In most of the cases, a shear thinning behaviour was observed in F4M, as these ratios were <0.9. A shear thickening behaviour seemed to be indicated for 5 Hz at the maximum strain, since the value of this ratio was clearly >1.1.

At this high frequency, clearly higher than that corresponding to the cross-over point, the sample was less able to relax when subjected to external stress. Thus, this shear thickening behaviour could be caused by

Table 4
Mean values of the ratios between the *minimum strain elastic modulus*, G'_M, and *large strain elastic modulus*, G'_L and the ratios between the *minimum strain rate viscosity*, $\dot{\eta}_m$, and the *large strain rate viscosity*, $\dot{\eta}_L$, for the three strain amplitude values chosen at the three frequencies considered, for both emulsions (F4M: hydroxypropyl methylcellulose; MX: methylcellulose). LSD are the least significant differences (n = 6).

Emulsion	Frequency (Hz)	Strain (%)	G'_L/G'_M	$\dot{\eta}_L/\dot{\eta}_m$
F4M	0.1	1	1.02^{C}	1.01^{BC}
		100	1.26^{C}	1.00^{BC}
		1000	17.22^{A}	0.82^{D}
	1	1	1.00^{C}	1.08^{B}
		100	1.09^{C}	1.05^{B}
		1000	8.60^{B}	0.94^{C}
	5	1	0.99^{C}	1.03^{BC}
		100	0.90^{C}	1.20^{A}
		1000	2.52^{C}	1.27^{A}
LSD			1.95	0.11
MX	0.1	1	0.98^{C}	1.12^{A}
		100	1.35^{BC}	0.89^{D}
		1000	4.83^{A}	0.9^{D}
	1	1	0.98^{C}	1.08^{AB}
		100	1.17^{BC}	0.90^{D}
		1000	4.51^{A}	1.05^{ABC}
	5	1	0.99^{C}	1.02^{AC}
		100	1.10^{C}	0.95^{CD}
		1000	2.03^{C}	0.99^{BCD}
LSD			0.90	0.11

^{ABC} For each emulsion, different letters in each column indicate significant differences between the means ($p < 0.05$) according to Fisher's test.

anisotropy at the interface. The droplet oriented itself before rupture and changed from its spherical shape (with the lowest surface/volume ratio). An increase in the interface occurred, leading to increased shear friction.

3.5. Strain hardening and shear thickening ratios

Strain-hardening (S) and shear-thickening (T) ratios were determined for the whole range of strain amplitudes considered. These ratios are considered as dimensionless indexs of nonlinearity (Wang & Selomulya, 2022). Their positive or negative values allow interpretation of their physical meaning. S > 0 shows intracycle strain stiffening, what means deformation rate decreases when increasing strain. S < 0 shows intracycle strain softening, i. e. deformation rate increases when increasing strain. On the other hand, T > 0 represents intracycle shear thickening (increasing viscosity with increasing strain rate) and T < 0 corresponds to intracycle shear thinning (decreasing viscosity with increasing strain rate) (Duvarci et al., 2017).

In Fig. 4, S and T ratios are represented as a function of the strain amplitude applied for both emulsions. Up to 100% strain, the S and T parameters of the different emulsions were equal to zero. This was in accordance with the linearity of elastic and viscous components and ellipsoid shape of Lissajous plots (Alghooneh, Razavi, & Kasapis, 2019). Beyond the linear region, S values increased to values above 1 for the three frequencies studied in both emulsions. It corresponded to intracycle strain stiffening (S > 0). T ratio decreased for the largest strains (T values < 0) in both emulsions. This result was indicative of shear thinning behaviour, in agreement with the flow curves in Fig. 1. F4M emulsion presented a shear thickening behaviour for 5 Hz, since the thickening ratio values turned to be positive. This fact was in accordance with the value of η_L/η_M >1 in Table 4 for 5 Hz and 1000%, and the curvature in viscous stress (dashed line) in Table 2.

The co-existence of strain-stiffening and shear thinning behaviour in hydrocolloid dispersions was explained by Alghooneh et al., 2019). The network structure breakdown involved stretching of polymer chains (strain stiffening), followed by breaking of interchain bonds, what resulted in chain slippage with each other (shear thinning). In the case of emulsions, this co-existence would be related to the elastic interface. The spherical droplets deform after stress is applied, becoming an ellipse and thus presenting a higher resistance to deformation (intrastrain stiffness). As the resulting ellipses are oriented in the direction of flow, friction decreases, as does viscosity (shear thinning).

LAOS properties for both emulsions were expected to be different, in accordance with the differences observed at rest (Fig. 2) and for small deformations and shear rates (Fig. 1). However, the non-linear parameters studied were quite similar in both emulsions as was the case of viscosity at high shear rates in flow curves. The reason for this result could be that the main difference in both emulsions was the type of cellulose. The different molecular weights resulted in different globule sizes in the emulsions, which affected the viscosity at rest and the microstructure, i.e. the SAOS parameters. In addition, results and properties at high shear rates or large deformations might be related to the structure breakdown mechanism, the rupture of the interface that would be alike in both emulsions and responsible for the similar MAOS-LAOS parameters calculated.

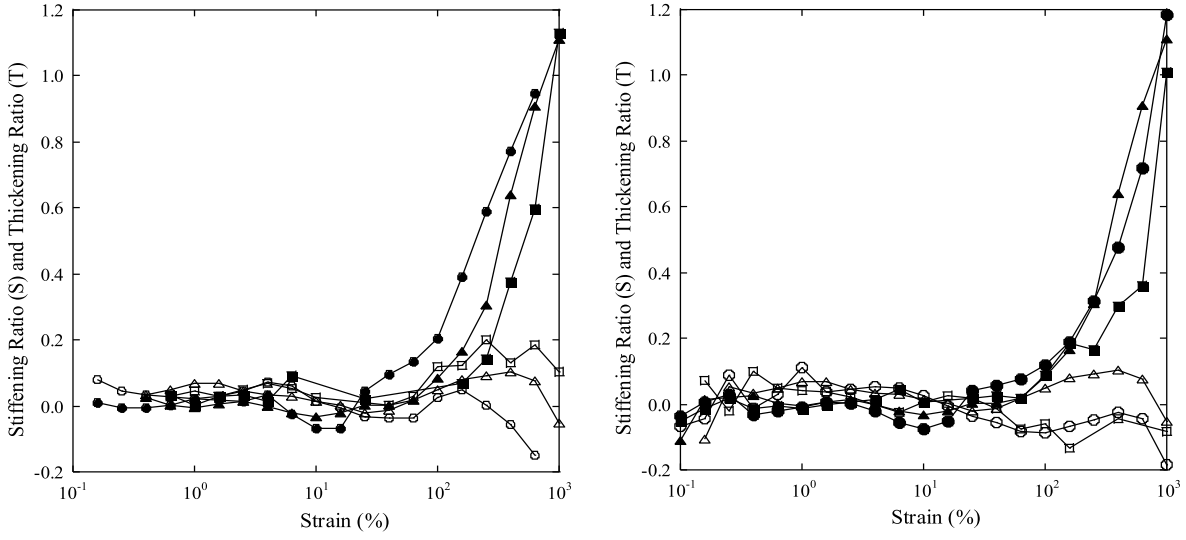

Fig. 4. Strain-stiffening ratio, S (filled symbols) and shear-thickening ratio, T (open symbols) as a function of oscillatory strain amplitude at the different frequencies studied (● 0.1 Hz, ▲1 Hz, ■5 Hz). **A**: Hydroxypropyl methylcellulose (F4M); **B**: Methylcellulose (MX).

4. Conclusions

This study is an example of the importance of the information reported when applying large deformations, providing results that may not be in accordance with those obtained in linear regime.

The different chemical structure of the two cellulose ethers had clear influence in the final emulsion structure characteristics and physical properties when considering small deformations and low shear rates. However, their rheological behaviour turned to be comparable when considering real conditions, such as manufacturing or oral processing.

Therefore, both could be used indistinctly in emulsions to be applied in food reformulation, although this was not expected from the initial characterization.

In conclusion, nonlinear viscoelastic analysis turns to be a fundamental and necessary tool for a complete and accurate textural characterization prior to final applications.

CRediT authorship contribution statement

M. Espert: Writing – original draft, Investigation, Data curation. **C. Gracia-Fernández:** Writing – review & editing, Methodology, Formal analysis. **A. Salvador:** Writing – review & editing, Resources, Funding acquisition. **T. Sanz:** Writing – review & editing, Resources, Funding acquisition. **M.J. Hernández:** Writing – review & editing, Supervision, Investigation, Formal analysis, Data curation, Conceptualization.

Declaration of competing interest

The authors of the article titled "**Linear and nonlinear viscoelasticity of edible o/w emulsions used as saturated fat replacers**" declare that there is no conflict of interest.

Data availability

The authors do not have permission to share data.

Acknowledgements

This work is supported by the Spanish Ministry of Science, Innovation and Universities (Funding number: PID2022-137587OB-C21). IATA-CSIC is a Centre of Excellence Severo Ochoa (CEX2021-001189-S funded by MCIN/AEI/10.13039/501100011033).

References

Aguilar-Zárate, M., Macias-Rodriguez, B. A., Toro-Vazquez, J. F., & Marangoni, A. G. (2019). Engineering rheological properties of edible oleogels with ethylcellulose and lecithin. *Carbohydrate Polymers, 205*, 98–105.

Alghooneh, A., Razavi, S. M., & Kasapis, S. (2019). Classification of hydrocolloids based on small amplitude oscillatory shear, large amplitude oscillatory shear, and textural properties. *Journal of Texture Studies, 50*(6), 520–538.

Anvari, M., & Joyner, H. S. (2017). Effect of fish gelatin-gum Arabic interactions on structural and functional properties of concentrated emulsions. *Food Research International, 102*, 1–7.

Arai, K., & Shikata, T. (2017). Hydration/dehydration behaviour of cellulose ethers in aqueous solution. *Macromolecules, 50*(15), 5920–5928.

Barnes, H. A. (2000). *A handbook of elementary rheology* (Vol. 1). Aberystwyth: University of Wales, Institute of Non-Newtonian Fluid Mechanics.

Borreani, J., Espert, M., Salvador, A., Sanz, T., Quiles, A., & Hernando, I. (2017). Oil-in-water emulsions stabilised by cellulose ethers: Stability, structure and in vitro digestion. *Food & Function, 8*(4), 1547–1557.

Borreani, J., Hernando, I., Salvador, A., & Quiles, A. (2017). New hydrocolloid-based emulsions for replacing fat in panna cottas: A structural and sensory study. *Journal of the Science of Food and Agriculture, 97*(14), 4961–4968.

Coblas, D., Broboana, D., & Balan, C. (2016). Correlation between large amplitude oscillatory shear (Laos) and steady shear of soft solids at the onset of the fluid rheological behaviour. *Polymer, 104*, 215–226.

Duvarci, O. C., Yazar, G., & Kokini, J. L. (2017). The comparison of Laos behaviour of structured food materials (suspensions, emulsions and elastic networks). *Trends in Food Science & Technology, 60*, 2–11.

Espert, M., Borreani, J., Hernando, I., Quiles, A., Salvador, A., & Sanz, T. (2017). Relationship between cellulose chemical substitution, structure and fat digestion in o/w emulsions. *Food Hydrocolloids, 69*, 76–85.

Espert, M., Bresciani, A., Sanz, T., & Salvador, A. (2019). Functionality of low digestibility emulsions in cocoa creams. Structural changes during in vitro digestion and sensory perception. *Journal of Functional Foods, 54*, 146–153.

Espert, M., Hernández, M. J., Sanz, T., & Salvador, A. (2021). Reduction of saturated fat in chocolate by using sunflower oil-hydroxypropyl methylcellulose based oleogels. *Food Hydrocolloids, 120*, Article 106917.

Ethers, M. C. (1997). *Technical handbook*. Midland, MI, USA: Dow Chemical Company.

Ewoldt, R. H., Hosoi, A. E., & McKinley, G. H. (2008). New measures for characterizing nonlinear viscoelasticity in large amplitude oscillatory shear. *Journal of Rheology, 52*(6), 1427–1458.

Ewoldt, R. H., Hosoi, A. E., & McKinley, G. H. (2009). Nonlinear viscoelastic biomaterials: Meaningful characterization and engineering inspiration. *Integrative and Comparative Biology, 49*(1), 40–50.

Faber, T. J., Van Breemen, L. C. A., & McKinley, G. H. (2017). From firm to fluid–Structure-texture relations of filled gels probed under Large Amplitude Oscillatory Shear. *Journal of Food Engineering, 210*, 1–18.

Gibis, M., Schuh, V., & Weiss, J. (2015). Effects of carboxymethyl cellulose (CMC) and microcrystalline cellulose (MCC) as fat replacers on the microstructure and sensory characteristics of fried beef patties. *Food Hydrocolloids, 45*, 236–246.

Gunasekaran, S., & Ak, M. M. (2000). Dynamic oscillatory shear testing of foods—selected applications. *Trends in Food Science & Technology, 11*(3), 115–127.

Hong, J. S., Kong, H. J., Hyun, K., Bergfreund, J., Fischer, P., & Ahn, K. H. (2019). Rheological analysis of oil–water emulsions stabilized with clay particles by Laos and interfacial shear moduli measurements. *Rheologica Acta, 58*(8), 453–466.

Hong, X., Zhao, Q., Chen, J., Ye, T., Fan, L., & Li, J. (2022). Fabrication and characterization of oleogels and temperature-responsive water-in-oil emulsions based on candelilla (Euphorbia cerifera) wax. *Food Chemistry, 397*, Article 133677.

Hyun, K., Wilhelm, M., Klein, C. O., Cho, K. S., Nam, J. G., Ahn, K. H., et al. (2011). A review of nonlinear oscillatory shear tests: Analysis and application of large amplitude oscillatory shear (Laos). *Progress in Polymer Science, 36*(12), 1697–1753.

Jiang, Y., Liu, L., Wang, B., Yang, X., Chen, Z., Zhong, Y., et al. (2019). Polysaccharide-based edible emulsion gel stabilized by regenerated cellulose. *Food Hydrocolloids, 91*, 232–237. https://doi.org/10.1016/j.foodhyd.2019.01.028

Joyner, H. S., & Meldrum, A. (2016). Rheological study of different mashed potato preparations using large amplitude oscillatory shear and confocal microscopy. *Journal of Food Engineering, 169*, 326–337.

Laguna, L., Primo-Martín, C., Varela, P., Salvador, A., & Sanz, T. (2014). HPMC and inulin as fat replacers in biscuits: Sensory and instrumental evaluation. *LWT-Food Science and Technology, 56*(2), 494–501.

Lee, S. (2018). Utilization of foam structured hydroxypropyl methylcellulose for oleogels and their application as a solid fat replacer in muffins. *Food Hydrocolloids, 77*, 796–802.

Li, Q., Xu, M., Xie, J., Su, E., Wan, Z., Sagis, L. M., et al. (2021). Large amplitude oscillatory shear (Laos) for nonlinear rheological behaviour of heterogeneous emulsion gels made from natural supramolecular gelators. *Food Research International, 140*, Article 110076.

Marangoni, A. G., Van Duynhoven, J. P., Acevedo, N. C., Nicholson, R. A., & Patel, A. R. (2020). Advances in our understanding of the structure and functionality of edible fats and fat mimetics. *Soft Matter, 16*(2), 289–306.

Martínez-Cervera, S., Salvador, A., & Sanz, T. (2015). Cellulose ether emulsions as fat replacers in muffins: Rheological, thermal and textural properties. *LWT-Food Science and Technology, 63*(2), 1083–1090.

McClements, D. J. (2009). Biopolymers in food emulsions. In S. Kasapis, I. T. Norton, & J. B. Ubbink (Eds.), *Modern biopolymer science* (pp. 129–166). Academic press.

Melito, H. S., Daubert, C. R., & Foegeding, E. A. (2012). Creep and large-amplitude oscillatory shear behaviour of whey protein isolate/κ-carrageenan gels. *Applied Rheology, 22*(6).

Melito, H. S., Daubert, C. R., & Foegeding, E. A. (2013). Relating large amplitude oscillatory shear and food behaviour: Correlation of nonlinear viscoelastic, rheological, sensory and oral processing behaviour of whey protein isolate/κ-carrageenan gels. *Journal of Food Process Engineering, 36*(4), 521–534.

Mezger, T. (2020). *The rheology handbook*. Hannover: Vincentz Network.

Otoni, C. G., Lorevice, M. V., de Moura, M. R., & Mattoso, L. H. (2018). On the effects of hydroxyl substitution degree and molecular weight on mechanical and water barrier properties of hydroxypropyl methylcellulose films. *Carbohydrate Polymers, 185*, 105–111.

Razavi, S. M. A., Alghooneh, A., Behrouzian, F., & Cui, S. W. (2016). Investigation of the interaction between sage seed gum and guar gum: Steady and dynamic shear rheology. *Food Hydrocolloids, 60*, 67–76.

Reinheimer, K., Grosso, M., Hetzel, F., Kübel, J., & Wilhelm, M. (2012). Fourier Transform Rheology as an innovative morphological characterization technique for the emulsion volume average radius and its distribution. *Journal of Colloid and Interface Science, 380*(1), 201–212.

Sanz, T., Falomir, M., & Salvador, A. (2015). Reversible thermal behaviour of vegetable oil cellulose ether emulsions as fat replacers. Influence of glycerol. *Food Hydrocolloids, 46*, 19–27.

Shimada, R. T., Fonseca, M. S., & Petri, D. F. (2017). The role of hydroxypropyl methylcellulose structural parameters on the stability of emulsions containing Spirulina biomass. *Colloids and Surfaces A: Physicochemical and Engineering Aspects, 529*, 137–145.

Szopinski, D., & Luinstra, G. A. (2016). Viscoelastic properties of aqueous guar gum derivative solutions under large amplitude oscillatory shear (Laos). *Carbohydrate Polymers, 153*, 312–319.

Tarancón, P., Fiszman, S. M., Salvador, A., & Tárrega, A. (2013). Formulating biscuits with healthier fats. Consumer profiling of textural and flavour sensations during consumption. *Food Research International, 53*(1), 134–140.

Van den Berg, L., Van Vliet, T., Van der Linden, E., Van Boekel, M. A. J. S., & Van de Velde, F. (2007). Breakdown properties and sensory perception of whey proteins/polysaccharide mixed gels as a function of microstructure. *Food Hydrocolloids, 21*(5–6), 961–976.

Wang, Y., & Selomulya, C. (2022). Food rheology applications of large amplitude oscillation shear (Laos). *Trends in Food Science & Technology, 127*, 221–244.

Yazar, G., Duvarci, O. C., Erturk, M. Y., & Kokini, J. L. (2019). Laos (large amplitude oscillatory shear) applications for semisolid foods. In H. Joyner (Ed.), *Rheology of semisolid foods* (pp. 97–131). Cham: Springer.

Yousefi, A. R., & Razavi, S. M. (2015). Dynamic rheological properties of wheat starch gels as affected by chemical modification and concentration. *Starch-Stärke, 67*(7–8), 567–576.